Spectrochimica Acta Part B 66 (2011) 706–711

Contents lists available at SciVerse ScienceDirect

Spectrochimica Acta Part B

journal homepage: www.elsevier.com/locate/sab

Experimental investigation of the asymmetric charge exchange reaction in the Ar^+–Ni system in the afterglow of a pulsed glow discharge

Ihor Korolov [a,*], Gregor Bánó [a,b], Zoltán Donkó [a]

[a] Research Institute for Solid State Physics and Optics of the Hungarian Academy of Sciences, H-1525 Budapest, POB 49, Hungary
[b] Department of Biophysics, P J Šafarik University in Košice, 04001 Jesenna 5, Košice, Slovakia

ARTICLE INFO

Article history:
Received 15 July 2011
Accepted 23 September 2011
Available online 1 October 2011

Keywords:
Asymmetric charge transfer
Reaction rate constant
Superelastic collision
Glow discharge

ABSTRACT

We have carried out spectroscopic measurements in the afterglow of pulsed glow discharges in Ar and in He–Ar mixtures to investigate elementary processes between Ar^+ ions and Ni atoms. The emission spectra in the afterglow showed a possibility of asymmetric charge transfer excitation of Ni II levels lying up to 1.6 eV energy difference below the Ar^+ ion level. For the rate coefficient of this reaction between $Ar^+(^2P_{3/2})$ ions and Ni atoms we obtained a value $k_{CT} = 2.3\ (\pm 0.9) \times 10^{-9}\ cm^3\ s^{-1}$, for room temperature, $T = 300$ K, conditions. For the reaction involving $Ar^+(^2P_{1/2})$ ions our measurements made it possible to derive an upper bound of $k^*_{CT} \leq 3.3\ (\pm 1.6) \times 10^{-9}\ cm^3\ s^{-1}$. Via measuring the time-dependence of the intensities of several Ni II spectral lines with different upper level energies we also obtained an upper bound for the rate of the superelastic scattering of electrons with $Ar^+(^2P_{1/2})$ ions, as $k_{eQ} \leq 1.3\ (\pm 0.8) \times 10^{-9}\ cm^3\ s^{-1}$.

1. Introduction

Asymmetric charge transfer (ACT) reactions between ground state noble gas ions and metal atoms play an important role in many glow discharge applications, such as in hollow cathode sources [1,2], in different metal ion lasers (e.g. Ne–Cu^+, He–Ag^+, He–Au^+, He–Cu^+, He–Zn^+, etc.) [3–8], as well as in analytical plasma sources [9–12], both in glow discharge mass spectrometry (GD-MS) [13–15], and glow discharge optical emission spectroscopy (GD-OES) [16]. The plasma sources of GD instruments are mostly operated in argon buffer gas. Detailed understanding of the operation of these plasma sources requires sophisticated numerical modeling of the discharge plasmas, the accuracy of which depends critically on the correctness of the input parameters. To date, the lack of knowledge of ACT rate coefficients has prevented precise modeling predictions of the relative sensitivity factors (RSF) [17–19] in GD-MS and limited the accuracy of the calculated emission spectra in GD-OES.

In the ACT reaction, a ground state metal atom (M) is ionized and excited by an ion (A^+) in a single step:

$$A^+ + M \rightarrow A + M^{+*} + \Delta E. \quad (1)$$

Unlike other ionization processes (like Penning ionization, or electron impact ionization), the ACT between atomic species and atomic ions is a selective (nearly-resonant) mechanism. The process is most efficient for excited metal ion M^{+*} levels having an energy $0 \leq \Delta E \leq 1$ eV below the ground state energy of the noble gas ion A^+, with highest cross sections belonging to an energy difference $\Delta E \cong 0.1$–0.3 eV [20]. We note that during discharge operation noble gas ions may have significant kinetic energy that makes endoergic charge transfer possible as well [21]. This process cannot take place in the late afterglow.

Earlier rate coefficient measurements of ACT reactions between noble gas ions and metal atoms were mainly carried out with volatile metals, like Hg, Pb, Cd, Zn, or Tl [22–26]. There are very few rate coefficient and cross-section data available for other elements, that are difficult to evaporate, e.g. Cu, Fe, Ti, Ni, Mo, etc. For the Ne^+–Cu system, data have been published at ~2000 K [27]. Cross sections for the interaction of Xe^+ ions and various metals have been determined for a wide range of ion energies 1 eV $\leq \varepsilon \leq$ 5000 eV [28]. Experimental rate coefficient data for ACT reactions between Ar^+ ions and iron atoms, at thermal energies (~300 K), have been derived in our recent work [29], which combined plasma diagnostics methods and a kinetic model of the afterglow plasma, allowing monitoring of the temporal evolution of the densities of different plasma species. In this experiment iron vapor was created inside a discharge cell by cathode sputtering and its density was measured by atomic absorption spectroscopy. The rate coefficient of the reaction was evaluated from the emission intensity decay of Fe^{+*} lines pumped by the ACT process in He–Ar–Fe and Ar–Fe afterglow plasmas. This work has shown that the rate of the ACT reaction is an order of magnitude higher than the rate of the Penning ionization, confirming (in agreement with [30]) that the ACT reaction at certain conditions can play a significant role in the ionization balance in GD cells. This observation stresses the need for further studies concerning other elements,

* Corresponding author.
E-mail address: Ihor.Korolov@gmail.com (I. Korolov).

0584-8547/$ – see front matter © 2011 Elsevier B.V. All rights reserved.
doi:10.1016/j.sab.2011.09.004

where ACT is expected to be important and, indeed, the aim of the present paper is to investigate the ACT process in the $Ar^+ + Ni$ system.

Experimental (spectroscopic) evidence for the ACT reaction between Ar^+ ions and Ni atoms has already been presented in [31–34], however, the rate coefficient of the reaction has not been measured yet, to our best knowledge. As to theoretical efforts, the semi-classical calculations of ACT rate coefficients between these species resulted in a value of $k = 0.43 \times 10^{-9}\ cm^3 s^{-1}$ [30].

This paper, as mentioned above, is devoted to experimental investigations on the ACT reactions between argon ions [both $Ar^+(^2P_{3/2})$ and $Ar^+(^2P_{1/2})$] and nickel atoms, and the determination of the rate coefficient of these processes. In Section 2 we describe the experimental apparatus and the method of data acquisition. Section 3 presents and discusses the results, while Section 4 summarizes the work.

2. Experimental

The scheme of the experiments is displayed in Fig. 1. The discharge cell is situated in a chamber connected to a vacuum and gas filling system. The base pressure of the system is below 5×10^{-9} mbar. We use 6.0 purity argon and helium gases, which are further purified using liquid nitrogen traps and a VICI P100-2 purifier [29].

The discharge cell has two plane and two hollow cathode electrodes, made of nickel of purity 99+% (supplied by Goodfellow Ltd.). This electrode configuration provides proper conditions for the experiments for a wide range of the charge transfer reaction rate, which is not known prior to the experiments. At a low charge transfer rate establishing a high metal vapor density, using the hollow cathodes, is advantageous. At a high rate the charge transfer reaction can already take place within the hollow cathode cavities, and a low density of ground state metal vapor reaches the center of the reaction cell. Under these conditions the plane cathodes provide a higher metal atom density in the center. Data acquired during the exploration phase of our measurements indicated that using the plane cathodes is the better choice. These plane cathodes have an active surface of 50 mm (length) × 5 mm (width). The inner diameter and the length of the anode cavity are 15 and 70 mm, respectively. Discharge pulses of 1.8 ms length are established by a high-voltage power supply, at a repetition rate between 2 Hz and 15 Hz, to keep the temperature of the discharge cell (measured by a K-type thermocouple) constant at different currents.

The rate coefficient of the ACT reactions is measured in a stationary afterglow experiment in the following way. (1) Nickel vapor is generated by sputtering the cathodes situated in the discharge cell, and its density, [Ni], is measured in a time-resolved manner using atomic absorption spectroscopy (AAS). (2) The decay rate of the Ar^+ ion density is determined by emission spectroscopy: the intensities of ACT-excited spectral lines are acquired during the afterglow period. (3) The ACT reaction rate is determined from a simple mathematical model considering additional processes influencing the ion density.

2.1. Absorption and emission spectroscopy

The Ni vapor density inside the cell is determined by atomic absorption spectroscopy (AAS), using a 2 m focal length Zeiss PGS-2 spectrometer equipped with a 650 grooves/mm grating and a Hamamatsu (H7732P-11) photomultiplier tube. The signal from the tube is recorded in a time-resolved photon counting mode by an AMETEK multi channel scaler PCI-card. As a light source we use a nickel HC lamp (model Hamamatsu L233-28NQ), operated at a current of 5 mA. The light of the lamp is collimated by Lens A and focused on the entrance slit of the spectrometer by Lens C, as shown in Fig. 1 (Lens B is not used in this measurement).

The ground electronic state of Ni I (a^3F) consists of $J = 4$, 3 and 2 sublevels with energies 0, 0.165 and 0.275 eV, and there is also a metastable state (a^3D) with $J = 3$, 2 and 1 sublevels at energies of 0.0254, 0.109 and 0.212 eV, respectively. As all these states can lead to ACT reactions with argon ions, one needs to account for the total density of Ni atoms at these levels. This can be accomplished following two different approaches. The first possibility is to carry out absorption measurements to determine the populations of each of these levels independently. This approach suffers from the low intensity and low absorbance of some of the transitions in the investigated spectral region. The other approach is based on the theoretical consideration that the populations of the levels are linked via respective statistical weights $2J+1$ and Boltzmann factors e^{-E_i/k_BT} (where E_i is the energy of the "initial" state and $T \cong 300$ K for our conditions). This theoretical prediction gives the following ratios for the populations of the different states: $[a^3F_4]:[a^3F_3]:[a^3F_2]:[a^3D_3]:[a^3D_2]:[a^3D_1] = 1:0.001:10^{-5}:0.291:0.008:10^{-4}$. To test this theoretical prediction we have experimentally checked the ratio between the populations of the a^3F_4 and a^3D_3 states. The density of the a^3F_4 state was derived from absorption on the 232.003 nm and 228.998 nm lines (with oscillator

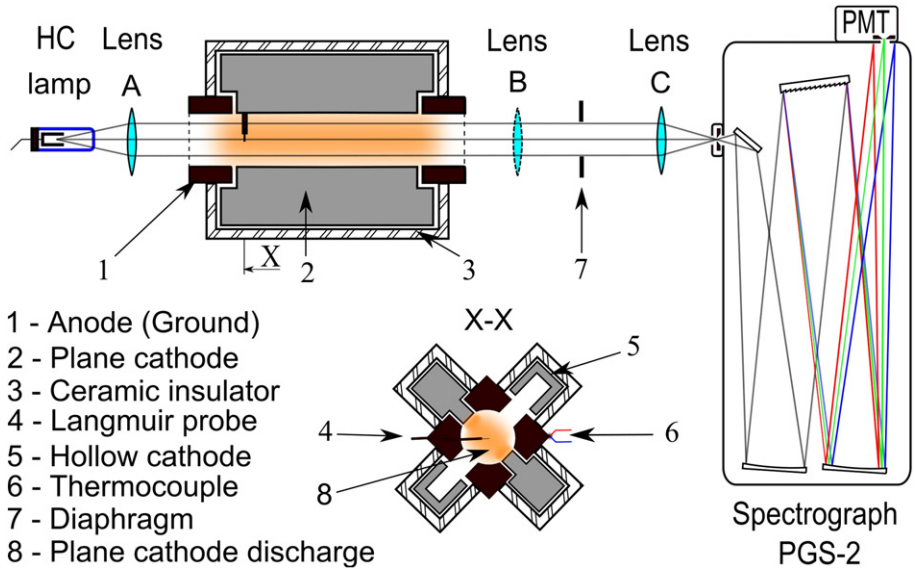

Fig. 1. Schematic view of the reaction cell and the optical setup. The X–X section is perpendicular to the optical axis.